

Safe, Occlusion-Aware Manipulation for Online Object Reconstruction in Confined Spaces

Yinglong Miao, Rui Wang, and Kostas Bekris

Rutgers University, New Brunswick, NJ, 08901, USA

Abstract. Recent work in robotic manipulation focuses on object retrieval in cluttered space under occlusion. Nevertheless, the majority of efforts lack an analysis of conditions for the completeness of the approaches or the methods apply only when objects can be removed from the workspace. This work formulates the general, occlusion-aware manipulation task, and focuses on safe object reconstruction in a confined space with in-place relocation. A framework that ensures safety with completeness guarantees is proposed. Furthermore, an algorithm, which is an instantiation of this framework for monotone instances, is developed and evaluated empirically by comparing against a random and a greedy baseline on randomly generated experiments in simulation. Even for cluttered scenes with realistic objects, the proposed algorithm significantly outperforms the baselines and maintains a high success rate across experimental conditions.

Keywords: interactive perception, manipulation, task and motion planning, object rearrangement, object reconstruction.

1 Introduction

Robotic manipulation has wide applications in manufacturing, logistics, and domestic domains. Unstructured scenes, such as logistics and home environments, require perception, mostly vision, for scene understanding [3]. Nevertheless, uncertainty in perception, such as occlusion, complicates the manipulation process. This work aims to address this issue, specifically, to safely reconstruct unknown objects online in a confined space and fully reveal the scene through in-hand sensing and in-place relocation, given a static RGB-D camera.

Such online object reconstruction is valuable functionality for manipulation in realistic scenarios where novel and unknown objects can appear frequently and challenge model-based methods [21]. Most applications, such as object retrieval in clutter and object rearrangement (e.g., setting up a dinner table), may require reconstructing only a subset of the objects in the scene. However, it is essential to understand how to reconstruct objects in these unstructured scenes with occlusion safely. Hence this work focuses on the case where all objects need to be reconstructed safely to completely reveal the scene while avoiding potential collisions. This helps achieve a foundational understanding of the object reconstruction domain and the conditions under which safety and some form of completeness can be achieved.

Addressing this task, however, can be challenging for a variety of reasons. For instance, robot reachability is quite limited in confined spaces, such as shelves, which complicates viable object placements and robot movements. Reachability constraints introduce dependencies between objects, which restrict the order with which objects can be manipulated safely [29]. On the other hand, with a single-camera view of the confined space, objects can often occlude each other, posing another constraint on the order of object movements, as occluded objects cannot be safely extracted without a known object model. These two challenges are interleaved and need to be solved simultaneously.

The majority of work in robot manipulation has assumed known object models [10,23,32,19]. More recently, the focus has shifted to cases where object models are unavailable. Nevertheless, most of these methods do not provide theoretical guarantees, either due to the dependence on machine learning [2,8,18,15], or assumptions that are valid only in limited scenarios [14]. Learning-based methods bring great promise to achieve efficiency but are highly desirable if they can be applied within a safe and complete framework. This work aims to provide such a framework on top of which more efficient solutions can be built.

In summary, this work first categorizes problems in object manipulation under occlusion and surveys past work in this field. Then, the task of safe object reconstruction in a confined space with in-place relocation is formalized. This formalization geometrically defines occlusion and the incurred object relationships. This leads to a probabilistically complete algorithmic framework with accompanying proof. The framework is general and can have different instantiations based on the implementation of primitives. An instantiation for monotone problems is proposed, which empirically shows significant improvements against a random and a greedy baseline in terms of computation time and number of actions taken, with a high success rate ¹.

2 Problem Classification and Related Work

The object manipulation problem belongs to the family of TAMP tasks [12], and past work has solved the object rearrangement task in a cluttered, and confined space [30,29]. To incorporate perception, Interactive Perception is a general methodology to benefit both domains [3,13]. Specifically for the task of object search and retrieval, [8] uses the POMDP framework to formulate the problem, namely the Mechanical Search problem. It has recently seen applications in different settings [18,15]. However, discussion of the general occlusion-aware manipulation tasks is still missing. In this section, this family of problems is categorized by different axes where challenges may occur to provide an overview.

Uncertainty Uncertainty in vision arises mainly in continuous uncertainty due to noise and discrete uncertainty due to occlusion. Many works have focused on continuous uncertainty. For instance, [31] explicitly models the uncertainty as a set of hypotheses and constructs a motion planner for a picking task. On the

¹ Code and videos can be found at <https://sites.google.com/scarletmail.rutgers.edu/occlusion-manipulation>.

other hand, discrete uncertainty can be modeled by geometric reasoning. This work focuses on this direction and assumes perfect sensing without continuous noise. Other works, however, do not explicitly model vision uncertainty but apply learning-based methods [27].

Workspace Confined space such as a shelf, which is handled in this work, is more constraining than a tabletop as in [32,26,25] since lateral access limits the valid grasp poses. Meanwhile, the clutteredness of the scene affects object placements [5,1]. On the other hand, objects can be physically unstable in unstructured scenes, such as heaps and piles [8,18]. The difficulty also depends on whether external buffers for object placement exist. When unlimited external buffers are provided, objects can be gradually extracted. Otherwise in-place arrangement is necessary which requires finding placement poses [11,5,1].

Object The assumptions on object models can involve known object models, category-level shape knowledge, or unknown object models. With known object models, objects are often assumed to be perfectly recognized once a part becomes visible [10]; or with the error modeled probabilistically [19]. Category-level knowledge can provide hints to estimate object models. For instance, when objects are cylinders, the pose and size can be estimated from visible parts [23]. When object models are unknown, objects may need to be reconstructed [21,14]. When the number of hidden objects is given, their poses can be sampled inside the occlusion region [2,32,19]. Otherwise, the scene needs to be fully revealed when it is unknown in the worst case. Lastly, the scene may include structures. For instance, an object can be stacked on top of the other, which constrains the sequence of movements [17,27].

Camera Mounting When the camera is fixed on the wrist of the robot, the robot needs to move the camera to reveal more space in the scene [2]. On the other hand, when the camera is static in the scene, the robot needs to bring objects in front of it for sensing, thus requiring more complicated actions.

Action Type A robot with a mobile base allows more reachability than a fixed base; non-prehensile actions allow more flexibility than prehensile actions. For object interactions, it is most constraining to prohibit object contacts. Otherwise, objects can be moved by contact with others, which is named Manipulation Among Moveable Obstacles [28].

Combinatorial Challenge One challenge that may arise is due to "monotonicity" as in object rearrangement [30]. A monotone problem is one where objects can be moved only once. Under partial observation, monotonicity can occur in several components. For instance, objects may need to be repeatedly moved to reveal a hidden object.

Model-Based Object Retrieval in a Shelf Many works in the literature focus on the problem of object search and retrieval with known object models from a shelf [10,23,2,32,19,15]. In this setting, The perception module is assumed to fully recognize the object once a sufficient part is observed, thus ignoring partial occlusion. [10] uses a graph to encode object occlusion and reachability dependencies and constructs an algorithm to solve the problem with a minimal number of actions. [23] encodes traversability of objects through a graph named

T-graph, which is specific to cylinders. The algorithm thus may not work for general objects. Both [10] and [23] remove objects from the scene, in which case completeness is trivial to satisfy.

Some other works rely on POMDP models [32,2,19], which can be solved by existing solvers or Reinforcement Learning (RL) algorithms. [19] explicitly models the trustworthiness of object recognition based on the occlusion ratio. [2] uses a learning-based method to sample target poses, which then guides a tree-search framework with an RL policy. [15] also uses learning-based estimators for the target object pose. Based on the estimation, a planner is constructed to find the best action. However, [15] limits actions to pushing left or right, and hence it can fail when pick-and-place actions are required.

This Work This work considers a more complicated task with unknown object models and focuses on safe object reconstruction with in-place relocation. [14], which is mostly related to this work, constructs a multi-step look-ahead algorithm that solves the object reconstruction problem completely in a grid-world scenario. However, it is not complete in realistic settings. Meanwhile, the system only relies on single-shot images without considering the observation history, hence having limited applications. This work instead explicitly combines past observations to update occlusion and object models.

Other Related Works Past work [21] uses TSDF [24] to reconstruct object models, which is adopted in this work. To ensure safety, this work models the object by a conservative volume and an optimistic volume following [22]. In-place object rearrangement is a hard problem as the simplified version of circle packing in 2D is shown to be NP-hard [9]. Recent work [5][1] sample placements and evaluate them based on reachability and blocking conditions, but limit to cylinder objects. Instead, this work applies to general-shaped objects by a novel convolution-based method to sample collision-free placements.

3 Problem Formulation

This section defines several notions to formulate the task. A workspace W is defined as the space inside the shelf where objects can occupy. It is composed of free space, collision space, and occlusion space. An object model is defined as the set of points occupied by the object. The ground-truth object model is denoted as $X_i(s_i)$, which indicates the set of points occupied by object i at pose s_i . As only an estimate of the object model is available during execution, two approximations are used: a conservative volume $X_i^{con}(s_i)$ which contains the space occluded or occupied by object i ; an optimistic volume $X_i^{opt}(s_i)$ which contains the revealed faces of object i . At any time, they satisfy $X_i^{opt}(s_i) \subseteq X_i(s_i) \subseteq X_i^{con}(s_i)$. $s^0(i)$ denotes the initial pose of object i . A robot is represented by its geometry $R(q)$, the set of points occupied by the robot at joint state q . A suction cup is used with two actions: attach and detach in this work. After attaching, the object is assumed to have a fixed transformation relative to the attached link until detached.

Occlusion A pinhole camera is fixed relative to the robot base, with position denoted as c . At each time, the space occluded by object i can be represented as

$$O_i(s_i) \equiv \{x : \exists \alpha \in (0, 1), \alpha(x - c) + c \in X_i(s_i)\}.$$

The total occlusion space at each time is $O = \bigcup_i O_i(s_i)$. The perception is done at a discrete-time after each manipulation action for simplicity. The occlusion space by object i at time t can be represented as

$$O_i(s_i, t) \equiv \{x : \exists \alpha \in (0, 1), \alpha(x - c) + c \in X_i(s_i)\}$$

which is generated from the RGBD image captured by the camera at time t . The total occlusion at time t is defined as $O(t) = \bigcup_i O_i(s_i, t)$. The occlusion space by object i up to time t given past observation history is then

$$O_i(s_i, 1..t) \equiv O_i(s_i, t) \cap \bigcap_{k=1}^{t-1} O(k).$$

The total occlusion space up to time t is $\bigcap_{k=1}^t O(k)$. An object is defined to be **fully revealed** at time t if its visible face does not intersect with $\bigcap_{k=1}^t O(k)$. It is **partially revealed** if part of the visible face is in occlusion. Otherwise, the object is **hidden**, i.e., the visible face is contained in occlusion.

The prehensile action is parameterized as (i, s_i, τ_i) , which encodes moving object i to pose s_i by robot trajectory τ_i . **safety** requires seen and unseen parts of objects and robots to not collide with occluded or occupied space. Collision avoidance for unseen parts is constraining and depends critically on the shape and pose of objects. As the study of safe extractions for a general-shaped object is not the focus of this work, an extraction direction perpendicular to the shelf opening is used, which already works for many scenarios. For safety, only fully revealed objects can be extracted; and objects need to be reconstructed before rearranged.

Problem Formulation The problem can be formulated as finding a sequence of actions $[(o_i, s_i, \tau_i)]$ such that the above safety constraints are satisfied at each time, all objects are fully reconstructed, and the occlusion is entirely removed at a finite time T , i.e., $O(T) = \emptyset$.

4 Algorithms and Analysis

This section defines a data structure to represent object dependencies and then illustrates a theoretical framework that attains probabilistic completeness. A concrete instantiation of the framework is then introduced to solve monotone tasks.

4.1 Occlusion Dependency Graph (ODG)

Our algorithm depends on a graph which represents visibility constraints among objects. To construct the graph, the occlusion relationship between objects needs

to be defined. Recall that the occlusion space of an object i is defined to be

$$O_i(s_i) \equiv \{x : \exists \alpha \in (0, 1), \alpha(x - c) + c \in X_i(s_i)\}.$$

Then for objects i and j at poses s_i and s_j , the part of j occluded by i can be defined as:

$$O_{ij}(s_i, s_j) \equiv \{x \in X_j(s_j) : \exists \alpha \in (0, 1], \alpha(x - c) + c \in X_i(s_i)\}.$$

Following this, object i at pose s_i is defined to **occlude** (directly or indirectly) another object j at pose s_j if $O_{ij}(s_i, s_j) \neq \emptyset$. As objects may jointly occlude a region, it is helpful to separate the occlusion contribution of each object. To achieve this, the **direct occlusion space** of an object i at pose s_i can be defined:

$$\begin{aligned} \tilde{O}_i(s_i) \equiv \{x : \exists \alpha \in (0, 1], \alpha(x - c) + c \in X_i(s_i), \\ \forall \beta \in (\alpha, 1), \forall k \neq i, \beta(x - c) + c \notin X_k(s_k)\}. \end{aligned}$$

In other words, it is the region where the camera ray does not pass through other objects after object i . Then the part of object j directly occluded by object i can be defined as

$$\begin{aligned} \tilde{O}_{ij}(s_i, s_j) \equiv \{x \in X_j(s_j) : \exists \alpha \in (0, 1], \alpha(x - c) + c \in X_i(s_i), \\ \forall \beta \in (\alpha, 1), \forall k \neq i, j, \beta(x - c) + c \notin X_k(s_k)\}. \end{aligned}$$

Similar as before, object i at pose s_i is defined to **directly occlude** j at pose s_j if $\tilde{O}_{ij}(s_i, s_j) \neq \emptyset$. The differences between occlusion space and direct occlusion space of an object are illustrated in Fig. 1.

Building on the above-defined notions, a directional graph can be built, which is named the **Occlusion Dependency Graph (ODG)**. In this graph, each node i represents the object i . Two nodes i and j are connected by edge (j, i) , if $\tilde{O}_{ij}(s_i, s_j) \neq \emptyset$, i.e. if object i directly occludes j . An example of the ODG is shown in Fig. 1, where a node C is included to represent the camera, and an edge (i, C) exists if part of object i is visible from the camera.

Safety constraints require the topological order of ODG to be followed so that only fully revealed objects are extracted first. The existence of such an order is guaranteed when the ODG is a Directed Acyclic Graph (DAG), which is the case when all objects are convex. However, having a topological order is not sufficient, as other objects can block extraction, and in-place relocation can modify the scene. To jointly tackle these challenges while following the topological order of the ODG, a theoretical framework is introduced in the following section.

4.2 A Probabilistically Complete Algorithm

The above challenges can be decoupled into the reachability and visibility challenges. The former involves finding valid object poses and motion planning of the robot, while the latter involves reconstructing objects and revealing occlusion. The following primitives can be introduced to tackle them individually:

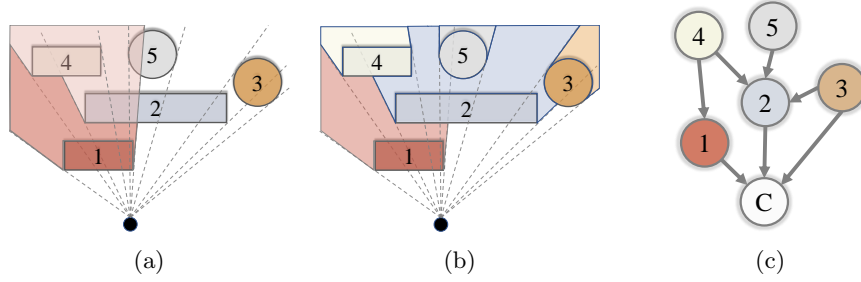


Fig. 1: Illustration of ODG. (a): Occlusion region and direct occlusion region of object 1. The dark red region indicates the direct occlusion region, while the occlusion region includes the light and the dark regions. (b): Direct occlusion region of each object. Each occlusion region is shown using a similar color as the corresponding object. (c): ODG of the objects. An edge (i, j) exists if object j directly occludes object i . C indicates the camera.

1. $reconstruct(i)$: this primitive extracts fully-revealed object i , reconstructs it, and places it back to its initial pose.
2. $reach_rearrange(V, i)$: this primitive rearranges objects in set V so that object i becomes reachable, and can be safely extracted.
3. $vis_rearrange(V, O)$: this primitive rearranges objects in set V so that part of the occlusion space O becomes revealed, and returns the revealed space.

These primitives are general and can be implemented in different ways in practice. Building upon them, a framework can be obtained to solve the problem as shown in Algorithm 1. This algorithm only reconstructs fully revealed objects and relocates objects after they are reconstructed. Hence it follows the topological order of ODG and ensures safety. The algorithm makes sure an object i is extractable by $reach_rearrange(V^*, i)$ where V^* is the set of reconstructed objects. It makes sure the direct occluded space of object i is revealed by $vis_rearrange(V^*, \tilde{O}_i(s_i^0))$, where $\tilde{O}_i(s_i^0)$ can be determined based on images. The algorithm postpones failed actions and attempts again when more space is revealed. However, it terminates when all actions fail, indicating the problem is unsolvable.

Lemma 1. *The algorithm defined in Algorithm 1 is probabilistically complete.*

Proof. If the algorithm finds a solution, the solution is correct, as it follows the topological order of ODG and reveals objects and occlusion safely through primitives. Conversely, if a solution exists, it can be converted to a sequence of the primitives mentioned above.

Denote (i_j, s_j, τ_j) as the j -th action in the solution, and denote the index of the first action applied to object i as $\pi(i)$. Since the solution must follow the

Algorithm 1: Target Extraction Under Occlusion Framework

```

1 init action queue  $Q = []$ , revealed objects  $V$ , and reconstructed objects  $V^* = \emptyset$ 
2 update action queue:  $Q = [reconstruct(i), \forall i \in V]$ 
3 while  $|V^*| \neq n$  do
4   If all actions in  $Q$  failed, then terminate as an infinite loop occurs, and
   the problem is unsolvable
5    $action \leftarrow Q.pop()$ 
6   if  $action == reconstruct(i)$  then
7     if  $reach\_rearrange(V^*, i) == FALSE$  then
8        $Q.push(reconstruct(i))$ 
9     else
10       $reconstruct(i)$ 
11       $V^* \leftarrow V^* \cup \{i\}$ 
12       $Q.push(vis\_rearrange(-, \tilde{O}_i(s_i^0)))$ 
13  if  $action == vis\_rearrange(-, O)$  then
14     $O' \leftarrow vis\_rearrange(V^*, O)$ 
15    if  $O' == \emptyset$  then
16       $Q.push(vis\_rearrange(-, O))$ 
17    else
18       $V' \leftarrow$  obtain newly revealed objects with revealed occlusion space
19       $Q.push(reconstruct(i)) \forall i \in V'$ 
20       $V \leftarrow V \cup V'$ 
21       $Q.push(vis\_rearrange(-, O \setminus O'))$ 

```

topological order of ODG, it can be reformulated as:

$$[(i_{\pi(1)}, s_{\pi(1)}, \tau_{\pi(1)}), (i_{\pi(1)+1}, s_{\pi(1)+1}, \tau_{\pi(1)+1}), \dots, \\ (i_{\pi(2)}, s_{\pi(2)}, \tau_{\pi(2)}), (i_{\pi(2)+1}, s_{\pi(2)+1}, \tau_{\pi(2)+1}), \dots, (i_{\pi(n)}, s_{\pi(n)}, \tau_{\pi(n)})]$$

As the solution is safe, $\{i_{\pi(k)+1}, i_{\pi(k)+2}, \dots, i_{\pi(k+1)-1}\}$ are objects that are reconstructed before object $i_{\pi(k+1)}$, hence only includes objects in $\{i_{\pi(1)}, \dots, i_{\pi(k)}\}$. To convert the actions to primitives, notice that $(i_{\pi(k)}, s_{\pi(k)}, \tau_{\pi(k)})$ can be converted into two actions:

$$(i_{\pi(k)}, s^0(i_{\pi(k)}), \tau_{\pi(k)}^1), (i_{\pi(k)}, s_{\pi(k)}, \tau_{\pi(k)}^2),$$

which puts object $i_{\pi(k)}$ back to its initial pose after reconstruction, and then to pose $s_{\pi(k)}$. The first action is equivalent to primitive $reconstruct(i_{\pi(k)})$. Hence

$$[(i_{\pi(k)}, s_{\pi(k)}, \tau_{\pi(k)})] \longrightarrow [reconstruct(i_{\pi(k)}), \tau_{\pi(k)}^1, (i_{\pi(k)}, s_{\pi(k)}, \tau_{\pi(k)}^2)].$$

After the conversion, as an object must be reachable before extracted, a dummy action $reach_rearrange(V^*, i_{\pi(k)})$ can be inserted before each $reconstruct(i_{\pi(k)})$ action. The action is dummy as the object is already reachable and nothing needs to be done. The object set V^* , as argued before, includes all reconstructed objects in $\{i_{\pi(1)}, i_{\pi(2)}, \dots, i_{\pi(k-1)}\}$. Hence

$$[reconstruct(i_{\pi(k)})] \longrightarrow [reach_rearrange(V^*, i_{\pi(k)}), reconstruct(i_{\pi(k)})].$$

Then any action that reveals part of $\tilde{O}_i(s_i^0)$ for some object i can be changed to $vis_rearrange(V^*, \tilde{O}_i(s_i^0))$, where V^* includes fully reconstructed objects at that time. For simplicity of analysis, it is safe to assume $reconstruct(i)$ only reconstructs object i but does not reveal occlusion, adding an extra action afterward. In such cases, $vis_rearrange(V^*, \tilde{O}_i(s_i^0))$ must be after $reconstruct(i)$.

After applying the above conversions, there may still be unconverted actions that do not reveal any part of occlusion. Since these actions must be applied to a reconstructed object at that time, it is safe to merge them to the next $reach_rearrange(\cdot, \cdot)$ or $vis_rearrange(\cdot, \cdot)$ primitive. After the above steps, the solution is changed to a sequence of primitives, which can be found by Algorithm 1 probabilistically and asymptotically as the number of iterations increases. Hence the algorithm is probabilistically complete.

The framework 1 is probabilistically complete but depends on two rearrangement primitives, which may run infinitely. A monotone algorithm is introduced in the following section to handle practical cases.

4.3 A Monotone Algorithm

The monotonicity in this task exists in two aspects: $vis_rearrange(\cdot, \cdot)$, when a single action cannot fully reveal an occluded space; and when objects need repeated moves to achieve the sampled placements. Algorithm 2 solves the case when both subproblems are monotone. The algorithm rearranges reconstructed objects so that the object to be extracted and reconstructed next is not blocked or visually occluded by others. Thus, the direct occlusion space can be fully revealed after extracting the object. As both reachability and visual occlusion are tackled in the rearrangement primitive, the algorithm defines a primitive $rearrange(i)$ that combines $reach_rearrange(V, i)$ and $vis_rearrange(V, O)$.

As illustrated in Figure 2 step (c), during rearrangement, the algorithm computes the sweeping volume and the vision cone in front of the object to check blocking objects and visual occlusion. If objects that have not been reconstructed exist in this region, then $rearrange(i)$ fails as they cannot be safely moved. Otherwise, the primitive rearranges all reconstructed objects in this region. It may also move other reconstructed objects outside this region to open space for placements. After that, It samples and verifies placements to avoid the computed region. Finally, a trajectory is found by motion planning and executed.

The primitive $reconstruct(i)$ decomposes the trajectory into a suction phase, an extraction phase, a sensing phase, and a placement phase. The suction phase computes a trajectory to move the manipulator to a valid suction pose. The extraction phase then extracts the object out of the shelf. The sensing phase completely reconstructs the object by a sequence of in-hand moves. Finally, the placement phase places the object back to its initial pose and resets the robot.

The algorithm guarantees that $\tilde{O}_i(s_i^0)$ is revealed when object i is reconstructed. Then following the topological order of ODG, it reconstructs all objects safely and reveals the entire scene. The algorithm is only probabilistically complete for monotone cases following a similar proof. However, experiments

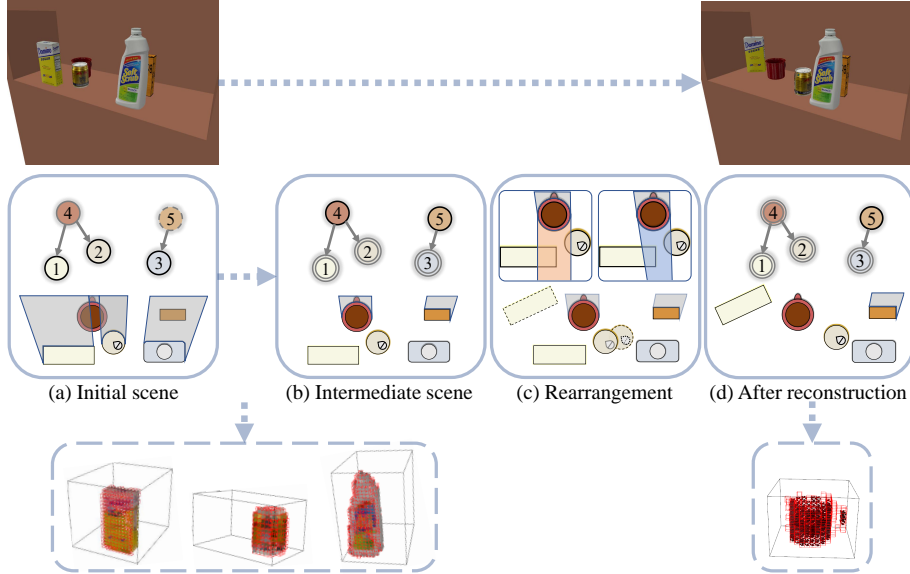


Fig. 2: The monotone algorithm in one iteration. 2D projection of objects and the ODG are illustrated. In (a), objects 1, 2, and 3 are fully revealed and highlighted in ODG. 5 is hidden and hence is dashed. 4 is partially occluded. After reconstructions of 1, 2, and 3, in (b), they are marked by double circles in ODG. 4 and 5 become fully revealed and hence highlighted. Before extracting 4, the sweeping volume shown in red in (c) and the vision cone shown in blue are visualized. The blocking objects 1 and 2 are rearranged by sampling placements. Then 4 is extracted and reconstructed, with the occlusion reduced as shown in (d).

show it can solve many practical tasks and perform better than the constructed baselines.

5 System Design

The system setup uses the left arm of a motoman robot with a suction gripper, which is of 8 DOF including the torsor joint, with a static RGBD camera. Voxels are used to model the workspace, where each voxel can be free, occupied, or occluded. The occlusion space of each object is computed given the depth and segmentation images by:

$$\hat{O}_i(s_i, t) = \{x : \phi(x) \in \phi(X_i(s_i)), d(x) \geq \text{depth}(\phi(x)).\}$$

Here $\phi(\cdot)$ denotes the projection of the 3D geometry on the 2D image; $d(x)$ denotes the depth of point x relative to the camera; and $\text{depth}(\phi(x))$ denotes the value of the depth image at the projected pixel $\phi(x)$. Given this, the net

Algorithm 2: Target Extraction Under Occlusion Monotone Algorithm

```

1 initialize reconstructed objects  $\bar{V} = \emptyset$ , failure count  $N_F = 0$ 
2 while  $|\bar{V}| \neq n$  do
3   visible objects  $S$ , revealed objects  $V$ , occlusion region  $\hat{O} \leftarrow \text{perception}()$ 
4    $i \leftarrow (V \setminus \bar{V})[0]$ 
5    $\text{rearrange}(i)$ 
6   status, newly revealed object set  $\tilde{V}$ , updated occlusion region  $\hat{O}$ , updated
   object model  $\hat{X}_i \leftarrow \text{reconstruct}(i)$ 
7   if  $\text{status} == \text{FAILURE}$  then
8      $V \leftarrow V[1:] \cup \{i\}$ ,  $N_F \leftarrow N_F + 1$ 
9   else
10    reset failure count  $N_F \leftarrow 0$ 
11     $V \leftarrow V \cup \tilde{V}$ ,  $\bar{V} \leftarrow \bar{V} \cup \{i\}$ 
12   if  $N_F == |V \setminus \bar{V}|$  then
13     return FAILURE

```

occlusion up to time t is obtained through the intersection of occlusion of each time. Each object is also modeled by voxels and TSDF for reconstruction [24]. Lastly, objects’ pixel positions and depth values are used to determine their occlusion relationship, which is sufficient for convex objects.

To sample viable placements in $\text{rearrange}(i)$, the system uses a novel method by convolution. It first projects the collision space and object geometry to 2D maps, then computes a convolution of them to obtain collision-free 2D placement poses. Samples are then drawn from this set and validated by IK and collision check. The system reconstructs an object by moving it to several waypoints outside the shelf. Waypoints are sampled such that the information gain (info-gain), computed as the volume of unseen space of the object, is maximized, similar to [16]. Fig. 3 illustrates the process, where the pose with the max info-gain is selected as the next waypoint.

The system uses PyBullet physics engine [7] to model the scene. The RGBD and segmentation images captured by the simulated camera are used for perception. Motion planning is achieved through MoveIt [6].

6 Experiments

6.1 Experimental Setup

A random and a greedy baseline are constructed for comparison. The random baseline uniformly samples objects to pick and locations to place them. The greedy one follows [14] by sampling choices of objects and placements and picking the action with the max info-gain, which is the volume of revealed occlusion. Both methods reconstruct objects before relocating them, and the greedy baseline prioritizes reconstruction actions if safe to do so. As they can run infinitely due to randomness, they are terminated once all objects are reconstructed or

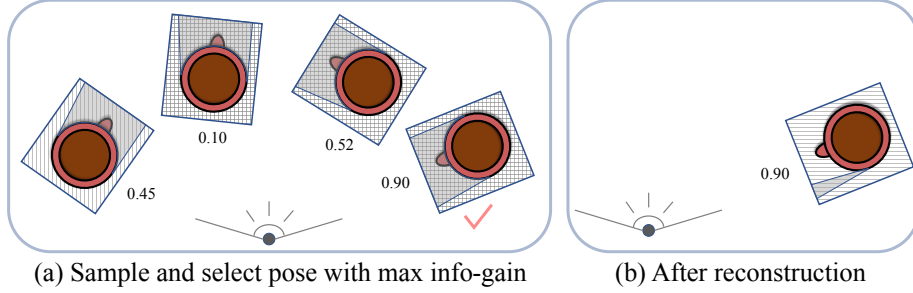


Fig. 3: Object reconstruction by sampling poses and computing info-gain. Sensing is done at several waypoints, each obtained through the process shown in the figure. Potential poses are first sampled with info-gain computed. Then the pose with the max info-gain is used as the next waypoint for sensing.

a timeout has been met. Hence the number of objects is given only in both baselines but not available in our algorithm.

The three algorithms are compared in a PyBullet simulated environment with random rectangular prisms and cylinders on the shelf. Experiments include three suites with 5, 8, or 11 objects. Each suite has three difficulty levels which are defined according to the size of objects. Objects are considered small if the width and length scale is 4cm or 5cm, medium if 7cm or 8cm, and large if 10cm or 11cm. Heights are randomly picked for each object from 9cm, 12cm, and 15cm. The easy level includes all small objects; the medium level includes 60% small, 30% medium, and 10% large objects; the hard level includes 25% small, 50% medium, and 25% large objects. Each scenario contains 10 randomly generated problem instances with at least one fully-hidden object. The instances are fixed across algorithms to allow fair comparison. A total of 5 trials of each algorithm is run for each instance to account for the randomness in the algorithm. Hence in total, there are 90 instances, with 450 total trials for each algorithm.

Easy, medium, and hard levels are denoted by indices 1, 2, and 3. Experiments are denoted as $n-k$ for n objects in the scene with difficulty level k . Due to a large number of trials, timeout is chosen as 250s for 5 objects; 350s, 400s, and 450s for 8-1, 8-2, and 8-3; and 500s, 600s, and 700s for 11-1, 11-2 and 11-3. It increases linearly as the difficulty level increases. Each trial is considered a success if all objects are reconstructed before the timeout and failed otherwise. For random and greedy algorithms, even when all objects are reconstructed, there is still a large space of occlusion in the scene unrevealed. Instead, our algorithm fully explores the environment at termination in most trails, which is illustrated in the remaining occlusion volume shown in Fig. 5. Beyond that, experiments also include YCB objects [4] obtained from [20] with 5 or 8 random objects. As the objects are larger than objects in simple geometry experiments, the scene with 11 objects is more cluttered and harder to solve, taking significantly more time. Hence YCB experiments with 11 objects are omitted and left for future work

Algo	5-1	5-2	5-3	8-1	8-2	8-3	11-1	11-2	11-3	ycb-5	ycb-8
random	68%	68%	54%	26%	16%	16 %	0 %	2%	8%	46%	10%
greedy	86%	68%	70%	38%	40%	36%	22%	14%	24%	84%	46%
ours	100%	100%	100%	100%	100%	94%	100%	100%	98%	96%	90%

Table 1: Success rate across scenarios. For tasks with rectangular prisms and cylinders, a total of 450 trials are run for each algorithm. For tasks with YCB objects, a total of 100 trials are run for each algorithm.

after the system is optimized. Each number of objects has 10 instances, and each instance is run for 5 trials². All experiments are run on an AMD Ryzen 7 5800X 8-Core Processor with 31.2GB memory.

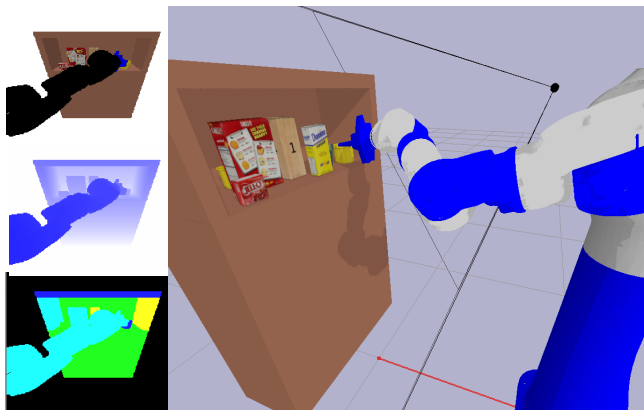


Fig. 4: Setup for 8 YCB objects. The experimental setup is similar for the other cases.

6.2 Results and Analysis

As shown in table 1, our algorithm achieves a near 100% success rate in all scenarios, consistently better than random and greedy algorithms given a large number of trials. The running time and number of actions of the three algorithms are illustrated in Fig. 5. Notice that the number of actions is at least the number of objects in the scene to reconstruct each object, but it may be more if they need multiple moves for rearrangement. Our method runs with less time and fewer actions and fully reveals the scene, consistently outperforming the two baselines.

² Code and videos can be found at <https://sites.google.com/scarletmail.rutgers.edu/occlusion-manipulation>.

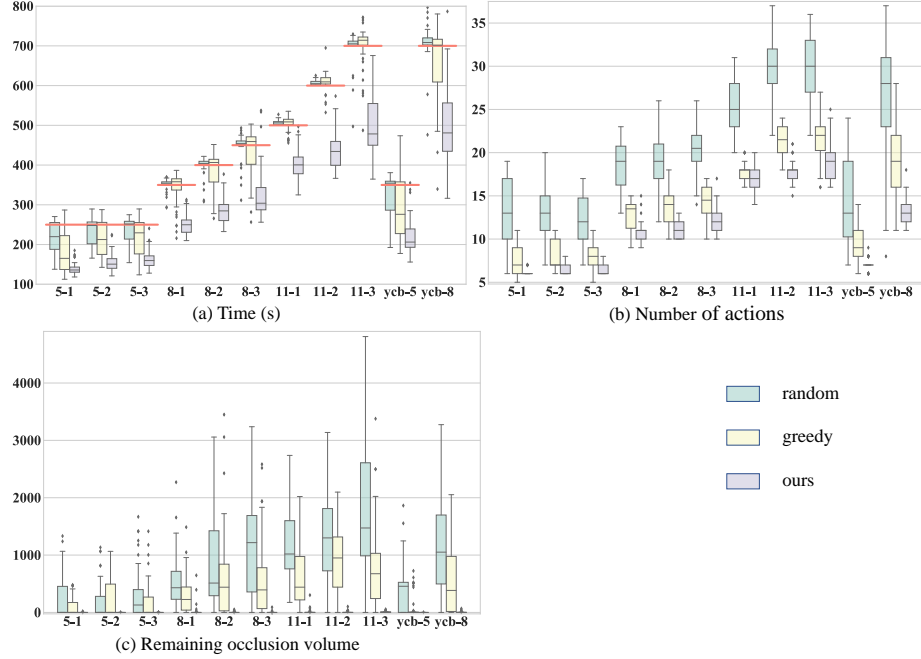


Fig. 5: Box plots showing running time (a), number of actions (b), and the remaining occlusion volume (c) of the algorithms. The red line in (a) indicates the predetermined timeout for each scenario to compute success ratio in Table 1.

Our algorithm is not optimized, which is left as future work. Time analysis is obtained for each component, including perception, motion planning, pose sampling, and rearrangement. Rearrangement takes more time as the difficulty increases, with time percentage ranging from 9% on 5-1 scenario to 30% on 11-3 scenario. The remaining time is spent mainly on motion planning and ROS communication, both taking roughly 30% of the rest. Pose generation and perception take 23% and 17% of the time without rearrangement. The number of calls to each component increases as the number of objects increases. Given this, the average time of each component can be derived, with 0.18s on average for perception, 0.86s for motion planning, 0.78s for pose generation, and 0.13s for ROS communication. Depending on the number of objects, each rearrangement call takes 10s to 37s across the experiments.

7 Conclusion and Future Work

This work surveys and categorizes the occlusion-aware manipulation task. It then focuses on the problem of safe object reconstruction in confined space with in-place relocation. It proposes a probabilistically complete framework with an

efficient algorithm instantiation for a subset of the task. The general combinatorial notion of monotonicity is also analyzed. Experiments in simulation show that our method attains a high success rate with less computational time and fewer actions than a random and a greedy baseline. As the current work focuses on problem formulation and completeness analysis, the optimization of each primitive component is left for future work. A more informed search can also optimize the algorithm to reduce the number of actions and submodule calls. Furthermore, this work will be integrated with perception primitives for object pose tracking and reconstruction to transfer to real-world platforms.

References

1. J. Ahn, J. Lee, S. H. Cheong, C. Kim, and C. Nam. An integrated approach for determining objects to be relocated and their goal positions inside clutter for object retrieval. In *ICRA*, pages 6408–6414, 2021.
2. W. Bejjani, W. C. Agboh, M. R. Dogar, and M. Leonetti. Occlusion-aware search for object retrieval in clutter. In *IROS*, pages 4678–4685, 2021.
3. J. Bohg, K. Hausman, B. Sankaran, O. Brock, D. Kragic, S. Schaal, and G. S. Sukhatme. Interactive perception: Leveraging action in perception and perception in action. *IEEE TRO*, 33(6):1273–1291, 2017.
4. B. Calli, A. Singh, A. Walsman, S. Srinivasa, P. Abbeel, and A. M. Dollar. The ycb object and model set: Towards common benchmarks for manipulation research. In *ICAR*, pages 510–517, 2015.
5. S. H. Cheong, B. Y. Cho, J. Lee, C. Kim, and C. Nam. Where to relocate?: Object rearrangement inside cluttered and confined environments for robotic manipulation. In *ICRA*, pages 7791–7797, 2020.
6. D. Coleman, I. Sucas, S. Chitta, and N. Correll. Reducing the barrier to entry of complex robotic software: a moveit! case study. *arXiv:1404.3785*, 2014.
7. E. Coumans and Y. Bai. Pybullet, a python module for physics simulation for games, robotics and machine learning. <http://pybullet.org>, 2016–2021.
8. M. Danielczuk, A. Kurenkov, A. Balakrishna, M. Matl, D. Wang, R. Martín-Martín, A. Garg, S. Savarese, and K. Goldberg. Mechanical search: Multi-step retrieval of a target object occluded by clutter. In *ICRA*, pages 1614–1621, 2019.
9. E. D. Demaine, S. P. Fekete, and R. J. Lang. Circle packing for origami design is hard. *arXiv:1008.1224*, 2010.
10. M. R. Dogar, M. C. Koval, A. Tallavajhula, and S. S. Srinivasa. Object search by manipulation. *Autonomous Robots*, 36(1):153–167, 2014.
11. K. Gao, D. Lau, B. Huang, K. E. Bekris, and J. Yu. Fast high-quality tabletop rearrangement in bounded workspace. In *ICRA*, 2022.
12. C. R. Garrett, R. Chitnis, R. Holladay, B. Kim, T. Silver, L. P. Kaelbling, and T. Lozano-Pérez. Integrated task and motion planning. *Annual Review of Control, Robotics, and Autonomous Systems*, 4:265–293, 2021.
13. C. R. Garrett, C. Paxton, T. Lozano-Pérez, L. P. Kaelbling, and D. Fox. Online replanning in belief space for partially observable task and motion problems. In *ICRA*, pages 5678–5684, 2020.
14. M. Gupta, T. Rühr, M. Beetz, and G. S. Sukhatme. Interactive environment exploration in clutter. In *IROS*, pages 5265–5272, 2013.

15. H. Huang, M. Dominguez-Kuhne, V. Satish, M. Danielczuk, K. Sanders, J. Ichnowski, A. Lee, A. Angelova, V. Vanhoucke, and K. Goldberg. Mechanical search on shelves using lateral access x-ray. In *IROS*, pages 2045–2052, 2020.
16. K. Huang and T. Hermans. Building 3d object models during manipulation by reconstruction-aware trajectory optimization. *arXiv:1905.03907*, 2019.
17. K. N. Kumar, I. Essa, and S. Ha. Graph-based cluttered scene generation and interactive exploration using deep reinforcement learning. In *ICRA*, 2022.
18. A. Kurenkov, J. Taglic, R. Kulkarni, M. Dominguez-Kuhne, A. Garg, R. Martín-Martín, and S. Savarese. Visuomotor mechanical search: Learning to retrieve target objects in clutter. In *IROS*, pages 8408–8414, 2020.
19. J. K. Li, D. Hsu, and W. S. Lee. Act to see and see to act: Pomdp planning for objects search in clutter. In *IROS*, pages 5701–5707, 2016.
20. Z. Liu, W. Liu, Y. Qin, F. Xiang, M. Gou, S. Xin, M. A. Roa, B. Calli, H. Su, Y. Sun, et al. Ocrtoc: A cloud-based competition and benchmark for robotic grasping and manipulation. *IEEE RA-L*, 7(1):486–493, 2021.
21. S. Lu, R. Wang, Y. Miao, C. Mitash, and K. Bekris. Online model reconstruction and reuse for lifelong improvement of robot manipulation. In *ICRA*, 2022.
22. C. Mitash, R. Shome, B. Wen, A. Boularias, and K. Bekris. Task-driven perception and manipulation for constrained placement of unknown objects. *IEEE RA-L*, 5(4):5605–5612, 2020.
23. C. Nam, S. H. Cheong, J. Lee, D. H. Kim, and C. Kim. Fast and resilient manipulation planning for object retrieval in cluttered and confined environments. *IEEE TRO*, 37(5):1539–1552, 2021.
24. R. A. Newcombe, S. Izadi, O. Hilliges, D. Molyneaux, D. Kim, A. J. Davison, P. Kohi, J. Shotton, S. Hodges, and A. Fitzgibbon. Kinectfusion: Real-time dense surface mapping and tracking. In *ISMAR*, pages 127–136, 2011.
25. T. Novkovic, R. Pautrat, F. Furrer, M. Breyer, R. Siegwart, and J. Nieto. Object finding in cluttered scenes using interactive perception. In *ICRA*, 2020.
26. A. Price, L. Jin, and D. Berenson. Inferring occluded geometry improves performance when retrieving an object from dense clutter. In *ISRR*, 2019.
27. A. H. Qureshi, A. Mousavian, C. Paxton, M. C. Yip, and D. Fox. Nerp: Neural rearrangement planning for unknown objects. In *RSS*, 2021.
28. M. Stilman, J.-U. Schamburek, J. Kuffner, and T. Asfour. Manipulation planning among movable obstacles. In *ICRA*, pages 3327–3332, 2007.
29. R. Wang, K. Gao, J. Yu, and K. Bekris. Lazy rearrangement planning in confined spaces. In *ICAPS*, 2022.
30. R. Wang, Y. Miao, and K. E. Bekris. Efficient and high-quality prehensile rearrangement in cluttered and confined spaces. In *ICRA*, 2022.
31. R. Wang, C. Mitash, S. Lu, D. Boehm, and K. E. Bekris. Safe and effective picking paths in clutter given discrete distributions of object poses. In *IROS*, 2020.
32. Y. Xiao, S. Katt, A. ten Pas, S. Chen, and C. Amato. Online planning for target object search in clutter under partial observability. In *ICRA*, 2019.